Paediatrics Publications   Paediatrics Department

Changes in the cardiac GHSR1a-ghrelin system correlate with myocardial dysfunction in diabetic cardiomyopathy in mice

Rebecca Sullivan
Lawson Health Research Institute

Rebecca McGirr
Lawson Health Research Institute

Shirley Hu
Western University

Alice Tan
Western University

Derek Wu
Western University

See next page for additional authors

Citation of this paper:

Authors

Rebecca Sullivan, Rebecca McGirr, Shirley Hu, Alice Tan, Derek Wu, Carlie Charron, Tyler Lalonde, Edith Arany, Subrata Chakrabarti, Leonard Luyt, and Savita Dhanvantari

Changes in the Cardiac GHSR1a-Ghrelin System Correlate With Myocardial Dysfunction in Diabetic Cardiomyopathy in Mice

Rebecca Sullivan,[1,2] Rebecca McGirr,[1] Shirley Hu,[3] Alice Tan,[2] Derek Wu,[2] Carlie Charron,[4] Tyler Lalonde,[4] Edith Arany,[2] Subrata Chakrabarti,[2] Leonard Luyt,[4,5,6] and Savita Dhanvantari[1,2,7]

[1]Imaging Research, Lawson Health Research Institute, London, Ontario N6A 4V2, Canada;
[2]Department of Pathology and Laboratory Medicine, Western University, London, Ontario N6A 4V2, Canada; [3]Department of Physiology and Pharmacology, Western University, London, Ontario N6A 3K7, Canada; [4]Department of Chemistry, Western University, London, Ontario N6A 5B7, Canada; [5]Departments of Oncology and Medical Imaging, Western University, London, Ontario N6A 4L6, Canada; [6]London Regional Cancer Program, Lawson Health Research Institute, London, Ontario N6A 4V2, Canada; and [7]Department of Medical Biophysics, Western University, London, Ontario N6A 5C1, Canada

Ghrelin and its receptor, the growth hormone secretagogue receptor 1a (GHSR1a), are present in cardiac tissue. Activation of GHSR1a by ghrelin promotes cardiomyocyte contractility and survival, and changes in myocardial GHSR1a and circulating ghrelin track with end-stage heart failure, leading to the hypothesis that GHSR1a is a biomarker for heart failure. We hypothesized that GHSR1a could also be a biomarker for diabetic cardiomyopathy (DCM). We used two models of streptozotocin (STZ)-induced DCM: group 1, adult mice treated with 35 mg/kg STZ for 3 days; and group 2, neonatal mice treated with 70 mg/kg STZ at days 2 and 5 after birth. In group 1, mild fasting hyperglycemia (11 mM) was first detected 8 weeks after the last injection, and in group 2, severe fasting hyperglycemia (20 mM) was first detected 1 to 3 weeks after the last injection. In group 1, left ventricular function was slightly impaired as measured by echocardiography, and Western blot analysis showed a significant decrease in myocardial GHSR1a. In group 2, GHSR1a levels were also decreased as assessed by Cy5-ghrelin(1–19) fluorescence microscopy, and there was a significant negative correlation between GHSR1a levels and glucose tolerance. There were significant positive correlations between GHSR1a and ghrelin and between GHSR1a and sarcoplasmic reticulum Ca^{2+}-ATPase 2a (SERCA2a), a marker for contractility, but not between GHSR1a and B-type natriuretic peptide, a marker for heart failure. We conclude that the subclinical stage of DCM is accompanied by alterations in the myocardial ghrelin-GHSR1a system, suggesting the possibility of a biomarker for DCM.

Diabetes affects ~6.5% of the population, or 347 million people worldwide, with this number expected to increase to 7.7%, or 439 million, by 2030 [1]. Cardiovascular disease affects ~80% of people with diabetes, and it is the major cause of morbidity and mortality. Diabetic cardiomyopathy (DCM) is a specific clinical condition characterized by progressive cardiac dysfunction without extensive coronary artery disease or hypertension [2]. The early stages of DCM represent a latent subclinical phase marked by diastolic dysfunction, oxidative stress,

derangements in Ca^{2+} homeostasis, and altered substrate utilization, resulting in myocardial lipotoxicity [3].

Ghrelin and its receptor, the growth hormone secretagogue receptor 1a (GHSR1a), are new molecules of interest that may track the progression of heart disease and the cardiomyopathy of diabetes. Ghrelin is a 28-amino-acid peptide hormone and is posttranslationally modified on Ser3 by octanoylation, a modification that is critical for binding to GHSR1a [4]. Both the acylated and nonacylated forms have been found in pericardial fluid [5], indicating that the human heart produces and secretes both forms. Both ghrelin and GHSR1a are present in the myocardium [6, 7] and may represent a ghrelin/GHSR1a system independent of the ghrelin/GHSR1a system that regulates energy expenditure. In myocardial tissue sections from patients with chronic heart failure (CHF), there were impaired ghrelin production and elevated GHSR1a levels, demonstrating that the ghrelin/growth hormone secretagogue receptor (GHSR) system is altered in end-stage heart failure [7]. Studies in ghrelin knockout mice have shown a role for ghrelin in the attenuation of left ventricular (LV) remodeling and excessive sympathetic activity after myocardial infarction [8, 9]. These cardioprotective effects of ghrelin may be mediated through activation of myocardial GHSR1a, as evidenced through signaling pathways that inhibit apoptosis [10] and promote angiogenesis (Akt phosphorylation), survival (adenosine 5′-monophosphate–activated protein kinase), and proliferation [extracellular signal–related kinase (ERK) phosphorylation] [11]. Activation of GHSR1a also regulates intracellular Ca^{2+} levels, and this mechanism may protect cardiomyocytes from ischemia/reperfusion injury [12] and preserve electrophysiological properties after myocardial infarction, thereby inhibiting apoptosis and promoting cell survival [13].

Although there is an established connection between myocardial ghrelin/GHSR and heart function and evidence that activation of ghrelin/GHSR1a signaling can prevent cardiac dysfunction after myocardial infarction [14, 15] and in CHF [16, 17], little is known about its expression and role in the progression of DCM. One recent study has shown that that treatment of diabetic mice with des-acyl ghrelin prevented cardiac dysfunction and cardiac fibrosis and enhanced signaling through adenosine 5′-monophosphate–activated protein kinase/ERK 1 and 2 [18]. However, des-acyl ghrelin does not bind GHSR1a [19]. To probe the relationship between cardiac ghrelin/GHSR and DCM, we examined changes in myocardial ghrelin and GHSR1a in mice with streptozotocin (STZ)-induced type 1 diabetes.

1. Materials and Methods

A. Animals

The Animal Use Subcommittee of the Canadian Council on Animal Care at Western University approved the protocols for all mouse handling and treatment procedures described in this study (protocols #2012-020 and #2015-097). There were two cohorts of mice in this study. Cohort 1 consisted of wild-type C57BL/6J female mice obtained from Jackson Laboratories at 5 weeks of age, which were randomly assigned to control (n = 6) or multiple low-dose STZ treatment (n = 6). Mice were injected intraperitoneally with 50 mg/kg STZ or with vehicle (sodium citrate buffer) once every other day for 3 days. Blood glucose readings (after a 4-hour fast) were taken 4 days before the first STZ injection and once per week for 10 weeks after the last STZ injection with a Bayer Ascensia Breeze 2 glucose meter and strips (Bayer HealthCare). Intraperitoneal glucose tolerance tests (IPGTTs) were conducted as described previously [20] 4 days before STZ treatment and 10 weeks after the last STZ injection. Briefly, fasting blood glucose readings were taken, and all mice were then injected intraperitoneally with 2 mg/kg of 40% dextrose. Blood glucose readings were taken 5, 25, 30, 60, and 90 minutes after injection. The area under the curve (AUC) for glucose tolerance tests was calculated with GraphPad Prism (GraphPad Software, Inc.).

Cohort 2 consisted of male and female nonobese diabetic/severe combined immunodeficient mice injected twice per day with vehicle (n = 8) or 35 mg/kg STZ (n = 6) at days 2 and 5 after

birth, as previously described for multiple low-dose STZ administration in neonatal mice [21]. At days 7, 14, 21, and 28 after STZ injection, IPGTTs were conducted after a 4-hour fast. Mice were euthanized immediately after IPGTT, and hearts were quickly removed, immersion-fixed in 4% paraformaldehyde, dehydrated in 30% sucrose (in phosphate-buffered saline), and snap-frozen in optimal cutting temperature compound for histological analyses. Because there were no apparent differences in AUC IPGTT values between the different time points, all STZ-treated mice were pooled into one treatment group.

B. Echocardiography

In cohort 1 mice, assessment of LV function was performed by echocardiography. Hair was removed from the abdominal region with Nair™ hair removal cream (Church & Dwight Co., Inc.). Mice were anesthetized with 0.2 mL/20 g body weight of ketamine hydrochloride (Bioniche) through intraperitoneal injection. Aquasonic 100 ultrasound transmission gel (Parker Laboratories, Inc.) was applied onto a 15-MHz linear transducer and the abdominal region of each mouse. Echocardiogram assessments were performed on a VisualSonics scanner, and images were acquired in M-mode in Vevo 2100 Imaging System Cardiac Package software (VisualSonics). Papillary muscle was used as a landmark for locating the left ventricle. Fifteen to 20 images 1.5 to 5 seconds in duration were captured per mouse. A representative image was selected for each mouse based on the edge clarity of the endo-cardium, which is the innermost layer of the myocardium. Following a standard protocol [22], we used measurement tools to determine anterior wall thickness, posterior wall thickness and LV dimensions in both systole [end systolic diameter (ESD)] and diastole [end diastolic diameter (EDD)] from three consecutive cardiac cycles. Heart rates were averaged over five cardiac cycles from M-mode images. Ventricular parameters were calculated with the following standard formulas: percentage fractional shortening = $[(EDD - ESD)/EDD] \times 100$; LV mass = $1.055 * [(\text{anterior wall thickness} + EDD + \text{posterior wall thickness})^3 - EDD^3]$, where 1.055 is the specific density of the myocardium; corrected LV mass = $(0.8 \times LV \text{ mass}) + 0.6$. Immediately after the imaging session, mice were euthanized by CO_2 overdose, and their hearts were collected. A small portion of the left ventricle was removed for histological staining, and the remainder was used for Western blot analysis of GHSR1a.

C. Insulin Measurements and Western Blot Analysis

For determination of circulating insulin levels, trunk blood was collected after euthanasia. Insulin levels in serum were measured by enzyme-linked immunosorbent assay (Luminex). Western blot analysis of GHSR1a was conducted as described previously [23], with 50 µg cardiac protein extract from control and STZ-treated mice. We used 5 µg of GHSR1a-expressing membrane as positive control. Membranes were incubated in anti-GHSR1a rabbit polyclonal antibody, followed by horseradish peroxidase–linked secondary antibody (Table 1) for 1 hour. Bands were visualized and quantified with the Chemi Genius Bio Imaging System (Syngene) and GeneSnap software (Syngene).

Table 1. Information on Primary and Secondary Antibodies Used

Antigen	Catalog #	Dilution	Host	RRID#
Ghrelin	sc-10359	1:100	Goat	AB_2111733
SERCA2a	ab3625	1:300	Rabbit	AB_303961
BNP	ab19645	1:1000	Rabbit	AB_445037
Alexa Fluor 488	A11055	1:500	Donkey anti-goat	AB_2534102
Alexa Fluor 594	A21207	1:500	Donkey anti-rabbit	AB_141637
GHSR1a	sc20748	1:500	Rabbit	AB_2232483
IgG horseradish peroxidase conjugated	ab7090	1:5000	Goat anti-rabbit	AB_955417

D. Immunofluorescence Microscopy

Hearts were frozen and embedded in optimal cutting temperature compound as previously described [19, 23] and sectioned at 7 μm with a cryostat. Immunofluorescence staining was conducted as previously described [19, 23], with primary polyclonal antibodies as listed in Table 1 for 1 hour at room temperature. Samples were rinsed 2× in phosphate-buffered saline and incubated for 2 hours at room temperature with Alexa Fluor 488 donkey anti-goat immunoglobulin G (IgG) (Table 1) to visualize ghrelin and the heart failure biomarker B-type natriuretic peptide (BNP), and Alexa Fluor 594 donkey anti-rabbit IgG (Thermo Fisher Scientific) (Table 1) to visualize sarcoplasmic reticulum Ca^{2+}-ATPase 2a (SERCA2a), a sarcoplasmic reticulum (SR) protein that regulates intracellular Ca^{2+} flux. GHSR1a was detected with a far-red ghrelin analog probe ([Dpr^3(octanoyl),Lys^{19}(Cy5)ghrelin (1–19)-amide, referred to for simplicity as Cy5-ghrelin(1–19)] for 30 minutes, as previously reported [19]. We have shown that this fluorescently labeled ghrelin peptide analog binds to GHSR1a with similar affinity to that of wild-type ghrelin and can be used to detect changes in GHSR1a [19]. Sections were washed and mounted with ProLong Gold Antifade (Life Technologies). Images were captured on a Nikon Eclipse TE2000-S fluorescent microscope. Five random fields of view were acquired for each of four sections per heart at 20× magnification (Nikon NIS Elements version BR 4.50.00; Nikon Instruments). Images were imported for analysis into FIJI version 1.49v, a distribution of ImageJ (National Institutes of Health). Fluorescence was quantified with a custom FIJI script that returns raw integrated density, representing protein expression levels, as previously reported [19, 24]. Data analyses were performed with an unpaired Student t test, a one-way analysis of variance with Tukey *post hoc* test, and Pearson correlation with significance set at $P < 0.05$.

E. Fibrosis Imaging

Heart tissue sections were stained with Masson trichrome stain with picric acid in collaboration with the Pathology Core Laboratory at London Health Sciences Centre. Sections were visualized with bright field microscopy at 200× magnification with a Zeiss Axioskop EL-Einsatz microscope (Carl Zeiss) and Northern Eclipse software (Empix Imaging Inc.).

2. Results

A. Measurements of Glucose Tolerance and Cardiac Function in Cohort 1 Mice

In adult female C57BL/6 mice treated with multiple low-dose STZ, there was a fourfold decrease in serum insulin levels ($P < 0.001$) 72 days after STZ injection. At this same time, there was a 68% ($P < 0.01$) increase in blood glucose and a 65% ($P < 0.01$) increase in AUC (Table 2), indicating mild fasting hyperglycemia and impaired glucose tolerance. Some parameters of cardiac function, as determined by echocardiography, were altered: there was a significant increase ($P < 0.01$) in percentage fractional shortening, the LV mass decreased by 40% ($P < 0.05$), and the ESD decreased by 27% ($P < 0.05$) in the STZ-treated mice (Table 3).

Table 2. Body Weights, Insulin, and Glucose Levels for Cohort 1

	Body Weight (g)	Serum Insulin (pg/mL)	Blood Glucose d0 (mM)	Blood Glucose d72 (mM)	AUC IPGTT d0	AUC IPGTT d72
Control	23.1 ± 0.2	718 ± 60	8.1 ± 0.2	7.8 ± 0.4	1090 ± 77	1220 ± 54
STZ	23.3 ± 0.2	179 ± 17[b]	8.4 ± 0.3	11.5 ± 0.9[a]	1128 ± 54	1864 ± 167[a]

Glucose measurements were taken before (d0) and after (d72) STZ administration of mice in cohort 1. Values are means ± SEM (n = 6).

[a]$P < 0.01$.

[b]$P < 0.001$.

Table 3. Echocardiographic Measurements for Cohort 1

	Control	STZ
Heart rate, bpm	326 ± 13	287 ± 26
Anterior wall thickness, mm	0.9 ± 0.05	0.9 ± 0.2
Posterior wall thickness, mm	0.8 ± 0.1	0.8 ± 0.1
LV EDD, mm	3.5 ± 0.2	3.2 ± 0.2
LV ESD, mm	2.8 ± 0.2	2.2 ± 0.2[a]
LV mass, corrected, mg	70.5 ± 5.7	50.5 ± 5.7[a]
Fractional shortening, %	21.7 ± 1.1	32.6 ± 2.6[b]

Echocardiograph measurements were conducted 16 weeks after STZ injection before time of euthanasia in cohort 1. Values are means ± SEM (n = 6).

[a]$P < 0.05$.

[b]$P < 0.01$.

There were no differences in the heart rate, the anterior or posterior wall thickness, or the EDD (Table 3). Therefore, these mice showed some changes in LV function that were concomitant with mild fasting hyperglycemia and impaired glucose tolerance after treatment with STZ.

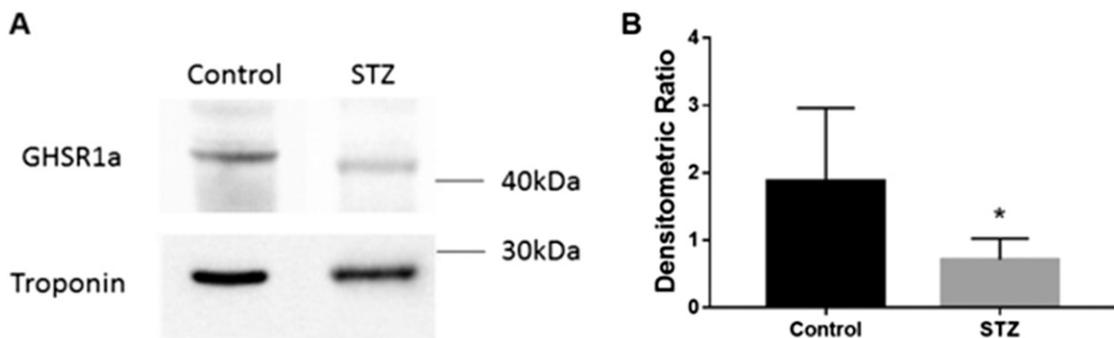### B. Expression of Cardiac GHSR1a in STZ-Treated Mice

Myocardial GHSR1a was assessed through Western blot analysis with the excised hearts of mice in cohort 1. Western blot analysis showed distinct bands corresponding to the molecular weight of GHSR1a (44 kDa) and cardiac troponin I (24 kDa), used as a positive control (Fig. 1A). A 2.6-fold ($P < 0.05$) decrease of GHSR1a (Fig. 1B) was seen in mice treated with STZ.

### C. Presence of Cardiac Fibrosis in Mouse Heart Tissues

The extent of cardiac fibrosis was detected in the hearts of mice in cohort 1 with histology and Masson trichrome stain. Representative images (Fig. 2A, 2B) show no apparent changes in the amounts of fibrotic tissue (blue) compared with the healthy tissue (red) in the STZ-treated mice vs. the control mice.

D. Glucose Tolerance of High-Dose STZ-Treated Mice

Neonatal mice from cohort 2 were treated with multiple low-dose STZ (35 mg/kg twice per day on day 2 and day 5 after birth) to induce diabetes in an acute manner. Body weights, blood

Figure 1. Changes in levels of myocardial GHSR1a in STZ-induced diabetes in cohort 1. (A) Western blot analysis of GHSR1a in control and STZ-treated mice with cardiac troponin as control. (B) Quantification of Western blot analysis, where data are represented as densitometric ratios of GHSR1a to cardiac troponin. Data are expressed as mean ± standard error of the mean (SEM) (n = 6). *$P < 0.05$.
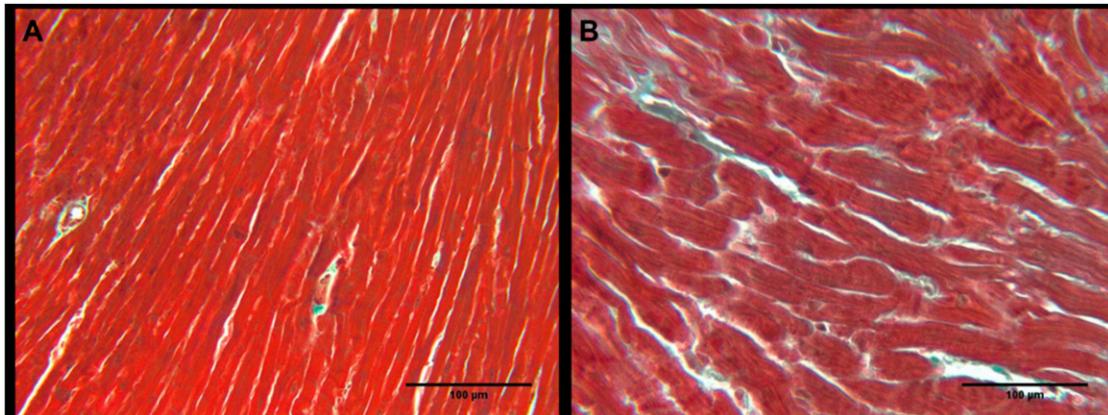
Figure 2. Cardiac fibrosis in (A) control and (B) STZ-treated mice from cohort 1. Representative images where blue is increased collagen deposition and red is healthy cardiac tissue.

glucose, and the AUC were measured before euthanasia (Table 4). The body weights of STZ-treated mice were not significantly different when compared with those of control mice. Fasting blood glucose levels increased 2.9-fold ($P < 0.01$) in the mice treated with STZ, and the AUC increased 4.2-fold ($P < 0.0001$).

E. Quantitative Fluorescence Microscopy of GHSR1a, Ghrelin, and Other Metabolic Markers of Heart Function

The expression of GHSR1a and other metabolic markers were measured in cardiac tissue sections from cohort 2. We have previously characterized Cy5-ghrelin(1–19) for its binding to and quantification of GHSR1a *in situ* [19]. Here, Cy5-ghrelin(1–19) was used to quantify the expression of GHSR1a, and immunofluorescent microscopy was used to determine the expression of ghrelin, BNP, and SERCA2a. BNP is a known biomarker for heart failure [25, 26], and SERCA2a regulates Ca^{2+} flux from the SR and is altered in diabetes [27]. Representative images of heart tissue from control (Fig. 3A–3D) and STZ-treated mice (Fig. 3E–3H) qualitatively show a decrease in the expression of GHSR1a and SERCA2a. Quantification of the fluorescent images (Fig. 3I) shows a 63% ($P = 0.0042$) decrease in expression of GHSR1a and an 85% ($P = 0.0015$) decrease in SERCA2a levels in hearts of diabetic mice. There was no difference in BNP or ghrelin expression between the control and STZ-treated mice.

F. Correlations Between GHSR1a, Ghrelin, BNP, and SERCA2a Expression in Mouse Cardiac Tissue

The quantified fluorescent data were used to determine possible relationships between the metabolic markers and glucose tolerance (AUC). There were significant negative correlations between AUC and GHSR1a ($r = 0.6632$, $P = 0.0097$) and AUC with SERCA2a ($r = 0.6508$, $P = 0.0117$) (Fig. 4). There were no significant correlations between AUC and ghrelin or BNP.
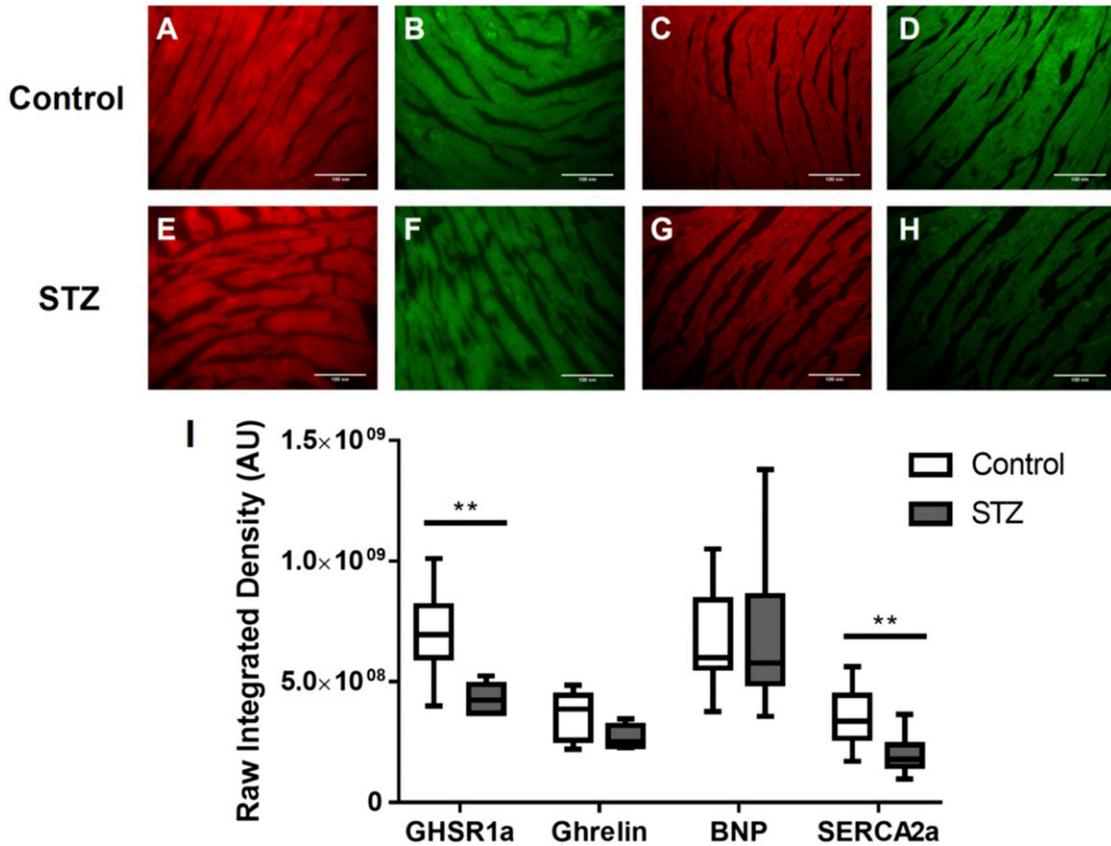
Table 4. Body Weights, AUC, and Glucose Levels for Cohort 2

	Body Weight (g)	Blood Glucose After STZ (mM)	AUC IPGTT After STZ
Control	21.7 ± 0.7	6.8 ± 0.5	890.2 ± 64
STZ	18.5 ± 1.5	19.7 ± 3.2[a]	3745 ± 87[b]

=Glucose measurements were taken 1 to 4 weeks after STZ administration of mice in cohort 2. Values are means ± SEM (n = 8 control, n = 6 STZ).
[a]$P < 0.01$.
[b]$P < 0.0001$.

Figure 3. Fluorescence microscopy analysis of GHSR1a, ghrelin, BNP, and SERCA2a in control and STZ-treated mice. Representative fluorescent images in cohort 2 of (A to D) control and (E to H) STZ-treated mice for GHSR1a, ghrelin, BNP, and SERCA2a. (I) Images were quantified as described in *Materials and Methods*. There were significant differences between control and STZ-treated mice in levels of GHSR1a and SERCA2a. Data are expressed as mean $\pm$ SEM based on independent t tests with significance set at $P < 0.05$. **$P < 0.01$.

Additional analysis examined relationships between metabolic markers. Interestingly, there was a highly significant positive correlation ($r = 0.7575$, $P = 0.0017$) between GHSR1a and ghrelin (Fig. 5A) and also between GHSR1a and SERCA2a ($r = 0.7154$, $P = 0.0040$) (Fig. 5C). In contrast, there was no significant interaction between GHSR1a and BNP (Fig. 5B). Interestingly, ghrelin and SERCA2a (Fig. 5D) also showed a strong positive correlation ($r = 0.8185$, $P = 0.0003$).

G. Presence of Cardiac Fibrosis in Mouse Heart Tissues

As for cohort 1, cardiac fibrosis was measured in cohort 2 via histology (Masson trichrome stain). Representative images (Fig. 6A, 6B) show no differences in the amount of fibrotic tissue (blue) compared with the healthy heart tissue (red) in the STZ-treated mice.

3. Discussion

In mouse models of type 1 diabetes, there is considerable evidence of cardiac dysfunction. In particular, in the STZ-induced mouse model, there are marked alterations in contractile function, accompanied by changes in cardiomyocyte Ca^{2+} homeostasis, increased oxidative stress, and altered substrate metabolism [28]. It is known that GHSR and ghrelin are expressed in the myocardium, and the expressions of both change in heart failure in humans
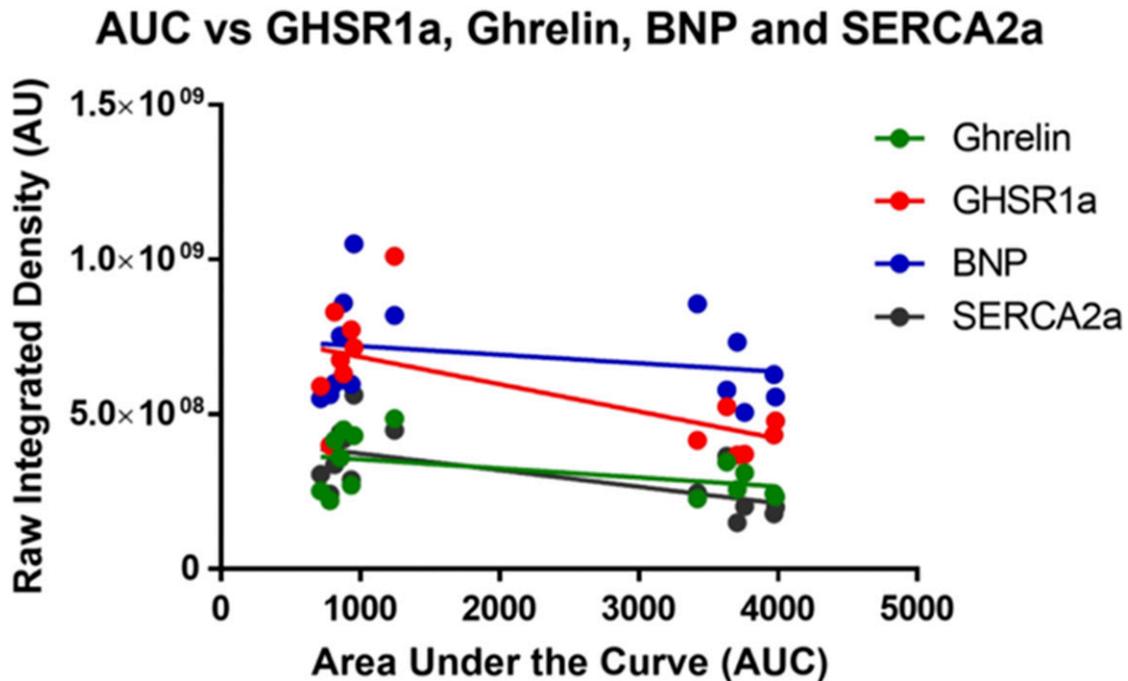
Figure 4. Correlation of GHSR, ghrelin, and BNP fluorescence intensities with glucose tolerance. Linear regression of ghrelin (green), GHSR1a (red), BNP (blue), and SERCA2a (gray) between the AUC and the raw integrated density. Each dot represents an individual animal, including both the control and the STZ-treated mice. There were significant negative correlations with glucose tolerance and GHSR1a ($P = 0.0097$, $r^2 = 0.6632$) and SERCA2a ($P = 0.0117$, $r^2 = 0.6508$) but not with ghrelin ($P = 0.0921$, $r^2 = 0.4672$) or BNP ($P = 0.8324$, $r^2 = 0.2548$).

[7]. In this study, we examined changes in levels of GHSR1a, along with changes in cardiac function or with known markers of DCM in mouse models of type 1 diabetes. Our major findings are that in both a chronic mild and an acute severe phenotype of type 1 diabetes, myocardial GHSR1a levels decreased before development of fibrosis. In the chronic, mild diabetic phenotype, the decrease in cardiac GHSR1a was accompanied by slight impairments in LV function. In the acute, severe diabetic phenotype, the decrease in GHSR1a did not correlate with a known marker of heart failure, BNP [25, 26]. However, levels of both GHSR1a and its ligand, ghrelin, did positively correlate with levels of SERCA2a, a marker of excitation-contraction coupling in cardiomyocytes. These results indicate that changes in GHSR1a expression may indicate changes in cardiac contractile function that characterize the subclinical phase of DCM.

The STZ-treated mouse has long been used as a model to study the progression and treatment of DCM [28]. Although high doses of STZ may induce effects on cardiomyocyte contraction independently of diabetes [29], administering STZ in multiple lower doses, as we did, may help avoid such effects. The multiple low-dose STZ model is attractive because of its ease of administration and the ability to induce diabetes quickly in different strains in both adult and neonatal mice, as we have done in the current study. As the current study and other studies [30] have shown, the STZ-treated mouse shows mild changes in LV function as measured by echocardiography, and there is very little indication that BNP, a marker of heart failure, or collagen type 1, a marker of fibrosis, are elevated. Instead, many changes occur in the biochemical pathways that lead to the development of DCM, such as increases in lipid oxidation, loss of contractility, and alterations in intracellular Ca^{2+} handling [28]. Therefore, it is an excellent model to study the subclinical changes that may precede overt DCM.

However, it is possible that the changes in myocardial GHSR1a that we observed in cohort 1 reflect a level of cardiac inflammation as a result of STZ administration. A recent report
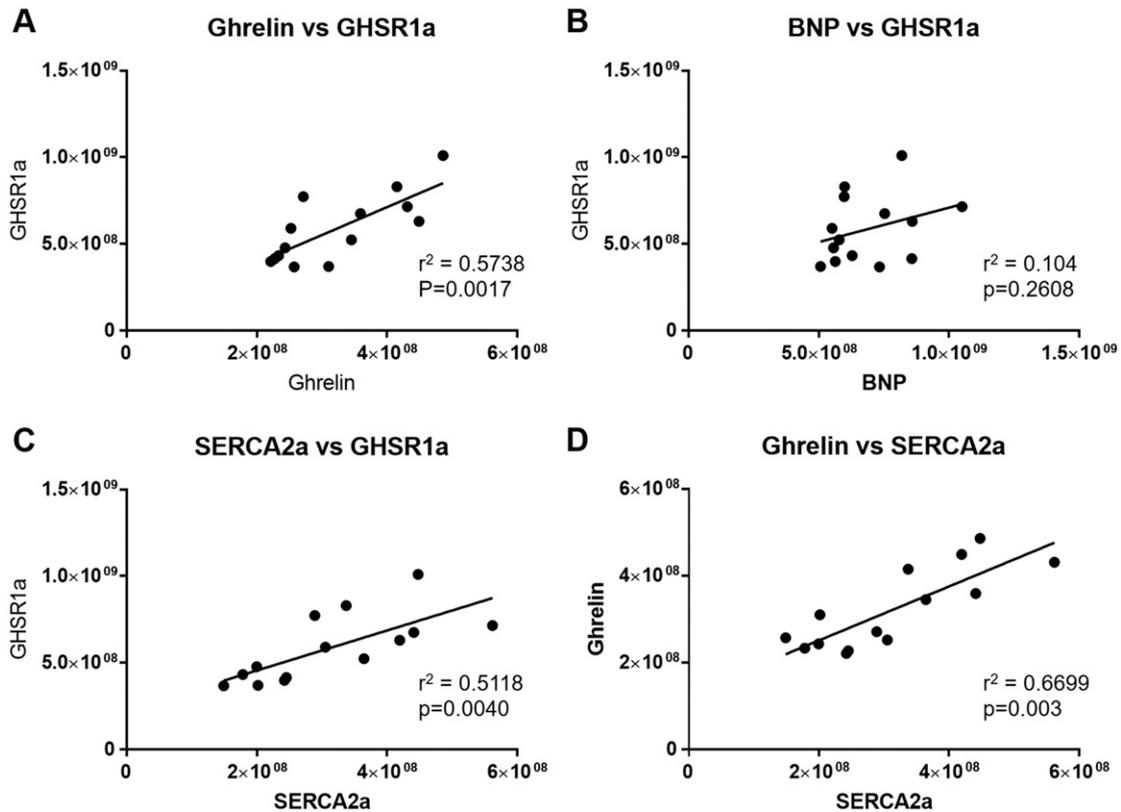
Figure 5. Correlational analyses of GHSR, ghrelin, BNP, and SERCA2a fluorescence intensities. Each point represents an individual mouse from either the control or STZ-treated group in cohort 2. There were significant interactions between (A) ghrelin and GHSR1a, (C) SERCA2a and GHSR1a, and (D) ghrelin and SERCA2a, but there was no significant correlation between (B) BNP and GHSR1a.

showed that multiple low-dose administration of STZ in adult male C57BL/6 mice upregulated markers of myocardial inflammation in the heart, including tumor necrosis factor-α, interleukin-6, interleukin-1β, and monocyte chemotactic protein-1, which coincided with increased cardiac fibrosis [31]. In contrast, we did not detect any appreciable fibrosis, indicating that it is unlikely that chronic inflammation was present. Nonetheless, we cannot rule out the
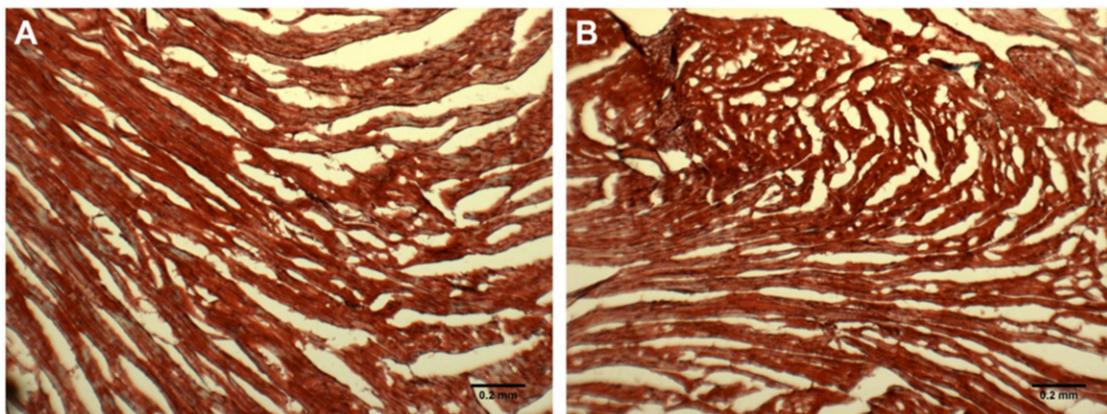
Figure 6. Cardiac fibrosis in (A) control and (B) STZ-treated mice from cohort 2. Representative images where blue is increased collagen deposition and red is healthy cardiac tissue.

possibility that there may be a very low level of inflammation preceding the onset of fibrosis and that changes in GHSR1a levels may be caused by such subclinical inflammation.

The primary significant correlation that was obvious from our study is that between both ghrelin and GHSR1a and SERCA2a, an SR membrane protein that transports intracellular Ca^{2+} into the SR during cardiomyocyte relaxation. The strong positive correlation suggests that GHSR1a activation by ghrelin may function to regulate cardiomyocyte contractility through control of Ca^{2+} flux from the SR. Evidence of a role for ghrelin in controlling Ca^{2+} flux through modulation of ion channels was shown in studies where ghrelin was administered to ventricular myocytes isolated from adult male rats [32]. Treatment with ghrelin increased the amplitude of the Ca^{2+} current through L-type voltage-gated Ca^{2+} channels, which was associated with increased cardiomyocyte contractility. However, whether ghrelin and GHSR1a also control Ca^{2+} flux at the level of the SR remains to be elucidated. This type of mechanism is especially pertinent to the progression of DCM; in diabetic rat hearts, decreased SERCA2a results in insufficient sequestration of Ca^{2+} in the SR, leading to impaired relaxation that characterizes the diastolic dysfunction of early DCM [27]. Conversely, overexpression of SERCA2a attenuates contractile dysfunction in STZ-treated mice [33]. Therefore, SERCA2a, and the associated proteins that control Ca^{2+} flux in the SR, are key regulators of myocardial contractility in DCM, and the ghrelin/GHSR system may be a biomarker for this mechanism.

The onset of cardiomyopathy has also been well characterized in the male Akita mouse model (*Ins2*^WT/C96Y^) of type 1 diabetes. In 3- and 6-month-old male Akita mice, there were no discernable changes in the LV echocardiographic parameters (ejection fraction, percentage fractional shortening, EDD or ESD); however, Doppler imaging showed early diastolic dysfunction with preserved systolic function [34]. These changes were accompanied by decreases in the levels of the signaling molecules Akt, ERK ½, and SERCA2a at 6 months of age, but there was no evidence of fibrosis. These effects were attributed to impaired signaling through the insulin receptor. Interestingly, both Akt and ERK 1/2 are also associated with cardiac GHSR1a signaling [10, 12], so it is likely that decreases in GHSR1a could also drive the reported decreases in phosphorylated Akt.

There may be a role for ghrelin as a possible biomarker for heart failure. In a study involving 145 patients with CHF, serum levels of ghrelin were significantly lower in patients with severe heart failure, and prognosis improved as serum ghrelin levels increased. Also, survival could be predicted based on a serum ghrelin level of >85 pM [35]. However, in DCM, serum ghrelin levels could be confounded by its role in energy balance. Plasma ghrelin levels increase dramatically in models of type 1 diabetes and can be suppressed by leptin infusion [36]. It is not known what effect these elevated circulating ghrelin levels would have on cardiac function and metabolism. Assuming that circulating ghrelin levels are elevated in our models, there could be negative feedback regulation of myocardial GHSR1a by circulating ghrelin. However, there is an intriguing possibility that the cardiac GHSR1a/ghrelin system functions independently of circulating ghrelin, because our results also show a decrease in the downstream signaling molecule, SERCA2a. These results suggest that myocardial GHSR1a is not activated in the face of high plasma ghrelin and instead may respond to autocrine activation. We are currently investigating this possibility.

Our results seem to indicate that cardiac tissue levels of ghrelin, together with GHSR1a, may be more appropriate markers of early cardiac dysfunction and may indicate changes in intracellular Ca^{2+} homeostasis in cardiomyocytes. Although we showed that a decrease in myocardial GHSR1a indicated the severity of impairment in glucose tolerance, a study involving tissue biopsies from 12 patients with CHF showed that both immunoreactive GHSR1a and GHSR1 AMRNA levels were dramatically increased in patients with end-stage heart failure [7]. Therefore, it appears that myocardial GHSR1a levels are altered differently in early-onset DCM and in end-stage heart failure. We are currently investigating a role for cardiac ghrelin and GHSR1a as an integrated system biomarker for the onset of DCM and heart failure.

Acknowledgments

References and Notes

1. Mozaffarian D, Benjamin EJ, Go AS, Arnett DK, Blaha MJ, Cushman M, de Ferranti S, Després J-P, Fullerton HJ, Howard VJ, Huffman MD, Judd SE, Kissela BM, Lackland DT, Lichtman JH, Lisabeth LD, Liu S, Mackey RH, Matchar DB, McGuire DK, Mohler ER III, Moy CS, Muntner P, Mussolino ME, Nasir K, Neumar RW, Nichol G, Palaniappan L, Pandey DK, Reeves MJ, Rodriguez CJ, Sorlie PD, Stein J, Towfighi A, Turan TN, Virani SS, Willey JZ, Woo D, Yeh RW, Turner MB; American Heart Association Statistics Committee and Stroke Statistics Subcommittee. Heart disease and stroke statistics—2015 update: a report from the American Heart Association. *Circulation.* 2015;**131**(4): e29–e322.

2. Miki T, Yuda S, Kouzu H, Miura T. Diabetic cardiomyopathy: pathophysiology and clinical features. *Heart Fail Rev.* 2013;**18**(2):149–166.

3. Boudina S, Abel ED. Diabetic cardiomyopathy, causes and effects. *Rev Endocr Metab Disord.* 2010; **11**(1):31–39.

4. Kojima M, Kangawa K. Ghrelin: more than endogenous growth hormone secretagogue. *Ann N Y Acad Sci.* 2010;**1200**(1):140–148.

5. Sax B, Merkely B, Túri K, Nagy A, Ahres A, Hartyánszky I, Hüttl T, Szabolcs Z, Cseh K, Kékesi V. Characterization of pericardial and plasma ghrelin levels in patients with ischemic and non-ischemic heart disease. *Regul Pept.* 2013;**186**:131–136.

6. Iglesias MJ, Piñeiro R, Blanco M, Gallego R, Diéguez C, Gualillo O, González-Juanatey JR, Lago F. Growth hormone releasing peptide (ghrelin) is synthesized and secreted by cardiomyocytes. *Cardiovasc Res.* 2004;**62**(3):481–488.

7. Beiras-Fernandez A, Kreth S, Weis F, Ledderose C, Pöttinger T, Dieguez C, Beiras A, Reichart B. Altered myocardial expression of ghrelin and its receptor (GHSR-1a) in patients with severe heart failure. *Peptides.* 2010;**31**(12):2222–2228.

8. Mao Y, Tokudome T, Otani K, Kishimoto I, Miyazato M, Kangawa K. Excessive sympathoactivation and deteriorated heart function after myocardial infarction in male ghrelin knockout mice. *Endocrinology.* 2013;**154**(5):1854–1863.

9. Soeki T, Kiddhimoto I, Schwenke DO, Tokudome T, Horio T, Yoshida M, Hosoda H, Kangawa K. Ghrelin suppresses cardiac sympathetic activity and prevents early left ventricular remodeling in rats with myocardial infarction. *Am J Physiol Heart Circ Physiol.* 2008;**294**(1):H426–H432.

10. Baldanzi G, Filigheddu N, Cutrupi S, Catapano F, Bonissoni S, Fubini A, Malan D, Baj G, Granata R, Broglio F, Papotti M, Surico N, Bussolino F, Isgaard J, Deghenghi R, Sinigaglia F, Prat M, Muccioli G, Ghigo E, Graziani A. Ghrelin and des-acyl ghrelin inhibit cell death in cardiomyocytes and endothelial cells through ERK1/2 and PI 3-kinase/AKT. *J Cell Biol.* 2002;**159**(6):1029–1037.

11. Yang C, Liu Z, Liu K, Yang P. Mechanisms of Ghrelin anti-heart failure: inhibition of Ang II-induced cardiomyocyte apoptosis by down-regulating AT1R expression. *PLoS One.* 2014;**9**(1):e85785.

12. Yuan MJ, Huang H, Huang CX. Potential new role of the GHSR-1a-mediated signaling pathway in cardiac remodeling after myocardial infarction (Review). *Oncol Lett.* 2014;**8**(3):969–971.

13. Ma Y, Zhang L, Launikonis BS, Chen C. Growth hormone secretagogues preserve the electrophysiological properties of mouse cardiomyocytes isolated from *in vitro* ischemia/reperfusion heart. *Endocrinology.* 2012;**153**(11):5480–5490.

14. Yuan M-J, Wang T, Kong B, Wang X, Huang C-X, Wang D. GHSR-1a is a novel pro-angiogenic and anti-remodeling target in rats after myocardial infarction. *Eur J Pharmacol.* 2016;**788**:218–225.

15. Huang C-X, Yuan M-J, Huang H, Wu G, Liu Y, Yu S-B, Li H-T, Wang T. Ghrelin inhibits post-infarct myocardial remodeling and improves cardiac function through anti-inflammation effect. *Peptides.* 2009; **30**(12):2286–2291.

16. Nagaya N, Uematsu M, Kojima M, Ikeda Y, Yoshihara F, Shimizu W, Hosoda H, Hirota Y, Ishida H, Mori H, Kangawa K. Chronic administration of ghrelin improves left ventricular dysfunction and attenuates development of cardiac cachexia in rats with heart failure. *Circulation*. 2001;**104**(12): 1430–1435.

17. Nagaya N, Miyatake K, Uematsu M, Oya H, Shimizu W, Hosoda H, Kojima M, Nakanishi N, Mori H, Kangawa K. Hemodynamic, renal, and hormonal effects of ghrelin infusion in patients with chronic heart failure. *J Clin Endocrinol Metab*. 2001;**86**(12):5854–5859.

18. Pei XM, Yung BY, Yip SP, Chan LW, Wong CS, Ying M, Siu PM. Protective effects of desacyl ghrelin on diabetic cardiomyopathy. *Acta Diabetol*. 2015;**52**(2):293–306.

19. Douglas GAF, McGirr R, Charlton CL, Kagan DB, Hoffman LM, Luyt LG, Dhanvantari S. Characterization of a far-red analog of ghrelin for imaging GHS-R in P19-derived cardiomyocytes. *Peptides*. 2014;**54**:81–88.

20. McGirr R, Hu S, Yee S-P, Kovacs MS, Lee T-Y, Dhanvantari S. Towards PET imaging of intact pancreatic beta cell mass: a transgenic strategy. *Mol Imaging Biol*. 2011;**13**(5):962–972.

21. Cox AR, Gottheil SK, Arany EJ, Hill DJ. The effects of low protein during gestation on mouse pancreatic development and beta cell regeneration. *Pediatr Res*. 2010;**68**(1):16–22.

22. Barouch LA, Berkowitz DE, Harrison RW, O'Donnell CP, Hare JM. Disruption of leptin signaling contributes to cardiac hypertrophy independently of body weight in mice. *Circulation*. 2003;**108**(6): 754–759.

23. McGirr R, McFarland MS, McTavish J, Luyt LG, Dhanvantari S. Design and characterization of a fluorescent ghrelin analog for imaging the growth hormone secretagogue receptor 1a. *Regul Pept*. 2011; **172**(1-3):69–76.

24. Guizzetti L, McGirr R, Dhanvantari S. Two dipolar α-helices within hormone-encoding regions of proglucagon are sorting signals to the regulated secretory pathway. *J Biol Chem*. 2014;**289**(21): 14968–14980.

25. Berger R, Huelsman M, Strecker K, Bojic A, Moser P, Stanek B, Pacher R. B-type natriuretic peptide predicts sudden death in patients with chronic heart failure. *Circulation*. 2002;**105**(20):2392–2397.

26. Maisel AS, Krishnaswamy P, Nowak RM, McCord J, Hollander JE, Duc P, Omland T, Storrow AB, Abraham WT, Wu AHB, Clopton P, Steg PG, Westheim A, Knudsen CW, Perez A, Kazanegra R, Herrmann HC, McCullough PA; Breathing Not Properly Multinational Study Investigators. Rapid measurement of B-type natriuretic peptide in the emergency diagnosis of heart failure. *N Engl J Med*. 2002;**347**(3):161–167.

27. Zhong Y, Ahmed S, Grupp IL, Matlib MA. Altered SR protein expression associated with contractile dysfunction in diabetic rat hearts. *Am J Physiol Heart Circ Physiol*. 2001;**281**(3):H1137–H1147.

28. Bugger H, Abel ED. Rodent models of diabetic cardiomyopathy. *Dis Model Mech*. 2009;**2**(9-10):454–466.

29. Wold LE, Ren J. Streptozotocin directly impairs cardiac contractile function in isolated ventricular myocytes via a p38 map kinase-dependent oxidative stress mechanism. *Biochem Biophys Res Commun*. 2004;**318**(4):1066–1071.

30. Mano Y, Anzai T, Kaneko H, Nagatomo Y, Nagai T, Anzai A, Maekawa Y, Takahashi T, Meguro T, Yoshikawa T, Fukuda K. Overexpression of human C-reactive protein exacerbates left ventricular remodeling in diabetic cardiomyopathy. *Circ J*. 2011;**75**(7):1717–1727.

31. Feng B, Chen S, Gordon AD, Chakrabarti S. miR-146a mediates inflammatory changes and fibrosis in the heart in diabetes. *J Mol Cell Cardiol*. 2017;**105**:70–76.

32. Sun Q, Ma Y, Zhang L, Zhao Y-F, Zang W-J, Chen C. Effects of GH secretagogues on contractility and Ca2+ homeostasis of isolated adult rat ventricular myocytes. *Endocrinology*. 2010;**151**(9):4446–4454.

33. Trost SU, Belke DD, Bluhm WF, Meyer M, Swanson E, Dillmann WH. Overexpression of the sarcoplasmic reticulum Ca(2+)-ATPase improves myocardial contractility in diabetic cardiomyopathy. *Diabetes*. 2002;**51**(4):1166–1171.

34. Basu R, Oudit GY, Wang X, Zhang L, Ussher JR, Lopaschuk GD, Kassiri Z. Type 1 diabetic cardiomyopathy in the Akita (Ins2WT/C96Y) mouse model is characterized by lipotoxicity and diastolic dysfunction with preserved systolic function. *Am J Physiol Heart Circ Physiol*. 2009;**297**(6): H2096–H2108.

35. Chen Y, Ji XW, Zhang AY, Lv JC, Zhang JG, Zhao CH. Prognostic value of plasma ghrelin in predicting the outcome of patients with chronic heart failure. *Arch Med Res*. 2014;**45**(3):263–269.

36. Tsubone T, Masaki T, Katsuragi I, Tanaka K, Kakuma T, Yoshimatsu H. Leptin downregulates ghrelin levels in streptozotocin-induced diabetic mice. *Am J Physiol Regul Integr Comp Physiol*. 2005;**289**(6): R1703–R1706.